Received: 3 April 2025 | Revised: 29 May 2025 | Accepted: 4 June 2025 | Published online: 19 June 2025

REVIEW

Smart Wearable Technology
2025, Vol. 1, A1, 1–9 Pages
DOI: 10.47852/bonviewSWT52025846

BON VIEW PUBLISHING

Risk Appraisal and Protection Against the Adverse Effects of Electromagnetic Fields on Living Tissues and Near-Tissues Health Devices

Adel Razek[1,*]

[1]*Group of Electrical Engineering – Paris, University of Paris-Saclay and Sorbonne University, France*

Abstract: This contribution aims to analyze the hostile side effects of electromagnetic fields on living tissues as well as smart health tools that work in proximity to living tissues. These include medical intervention tools, wearable devices, and imaging scanners. The evaluation, control, and protection against these adverse effects are also targeted. The implicated physics and their corresponding ruling mathematics are highlighted and discussed. Mathematical modeling using discretized local 3D numerical tools allowed the design, control, and validation of the durability of the devices. These different themes are supported by illustrated cases and an overview of bibliographic examples. The results of the investigation illustrate that the physical events involved in the origins of radiation and stray fields, as well as their adverse effects on exposed materials and their protection, allow a thorough understanding and control of their management. Moreover, the corresponding mathematical formulations dictating the behaviors of the involved fields allow their assessment according to Responsible Attitude and One Health approaches that enable ecological biodiversity and ecosystem.

Keywords: electromagnetic fields, adverse effects, phenomena physics, ruling mathematics, imaging scanners, wearable devices, battery charging tools

1. Introduction

In modern societies, the increasing presence of tools for daily life, combined with an increased use of electromagnetic fields (EMFs), has improved human well-being. These tools, in addition to their expected functions, can disrupt this well-being. These disruptions can concern living tissues in general, health tools, and other devices. The living tissues concerned are linked to biodiversity according to the One Health approach [1, 2]. Such approach refers to adverse effects of an artificial device on living tissues of humans as well as those of other biodiversity partners and hence the required protection impact also all. The health tools worried mainly concern those that work in proximity to living tissues such as medical intervention tools, wearable devices [3–6], and imaging scanners [7, 8]. Other tools concerned are those necessary for daily comfort, safety, etc. [9–12]. The involved side effect disturbances are mainly related to electromagnetic (EM) dissipated losses and EMF radiations. In addition to such exposures, another mode of EMF noise could perturb tools using EMF in their functioning. This is related to the introduction of EMF-sensitive matters as magnetic or conductors in the EMF scenery of the tool, for example the case of magneto resonance imaging (MRI) scanner [13, 14].

The role of EMF in EM energy devices is mainly related to energy conversion, transfer, or both actions. Most of such actions involve at once expected outcomes and unwanted effects. The energy conversion mode involves mainly the transformations of EM to mechanical (movement, deformation, vibration, etc.), thermal, or chemical. In the case of energy transfer, wireless EMF mode is mainly involved, which comprises radiofrequency (RF) telecommunication as mobile phones or their tower antenna [15–19] as well as charging systems as inductive power transfer (IPT) devices including those aboard electric vehicle (EV) [20–23]. Note that the case of wireless battery charging involves both conversion and transfer of energies.

As mentioned above, conversion modes can be expected or side effects. For example, EM-mechanical conversions may involve expected torque from electric motor or unwanted vibrations. Similarly, EM-thermal conversion may be expected outputs from heating systems or unwanted heat losses in materials. The case of EM-chemical conversion may involve expected battery charging or unsolicited corrosion of conductor or insulation defects.

A large part of the cases cited above contain stray fields that do not participate in the expected actions and are responsible for side effects. Normally, the fields are contained in the matter, which allows an effective projected action. The stray fields are due to the imperfection of the matter's capacity to contain the fields and could be reduced through design and optimization skills. The part of persistent stray fields could be treated by shielding. The stray fields as well as their shielding are related to the topological and phenomenological characteristics of the devices or shields.

A worthy management objective is to enhance intended outcomes and decrease unintended effects. This could be achieved

*Corresponding author: Adel Razek, Group of Electrical Engineering – Paris, University of Paris-Saclay and Sorbonne University, France. Email: adel.razek@centralesupelec.fr

through a Responsible Attitude (RA) involving Eco-design, thus improving intended performances and reducing unwanted side effects responsible for disruptions of medical tools and living tissues not only for humans but also for all biodiversity reflecting the One Health (OH) approach. Generally, RA and OH are approaches related to the protection of biodiversity and the ecosystem in an ecological context (Ecology is the scientific study of the processes influencing the distribution and abundance of organisms, the interactions among organisms, and the interactions between organisms). Note that the RA and OH approaches could be applied to both radiating [24] and exposed [25] devices.

The following sections discuss the physics of EMFs, the corresponding mathematical equations, protection from exposure to EMFs, and examples of adverse effects of exposure to EMFs. This will be followed by a discussion and conclusions.

2. Governing Physics of EMFs

Regarding the role of EMF in EM energy devices, related to energy conversion or transfer and possible adverse effects on matters due to losses dissipation or exposure to radiated fields, the governing physical phenomena involved in these processes are concerned in this section.

The different magnetic and electric physical quantities are interconnected and formulated by the Maxwell equations as will be shown in Section 3 (governing equations). Actually, the magnetic and electric fields **H** (A/m) and **E** (V/m) are related to the magnetic and electric inductions **B** (Wb/m^2 = T) and **D** (C/m^2) by the magnetic permeability μ = **B/H** and the electric permittivity ε = **D/E**. And, the electric current density **J** (A/m^2) is related to the electric field by the electric conductivity σ = **J/E**. These magnetic and electric three-dimensional (3D) vectors **H, E, B, D,** and **J** are as abovementioned, interconnected by the Maxwell equations. **B, D**, and **J** characterize surface densities related to the matter parameters μ, ε, and σ (respectively in H/m, F/m, and S/m). These depend on the nature of the material and the pulsation frequency f (in Hz) of the fields. For a high magnetic parameter, μ with small air gaps the magnetic field is theoretically contained in the material. The electrical parameters ε and σ in the material behave according to the range of f as the ratio of σ to $\omega \times \varepsilon$ (in F/(m × s) = S/m) where $\omega = 2\pi f$. Thus for very small values of f, the dielectric effect ω. ε is negligible compared to the conductive effect σ and the matter behaves as conductor, while for very large values of f, $\omega \times \varepsilon >> \sigma$ and the material behaves as a dielectric. Moreover, in conductive materials the distribution of induced currents is closely related to the frequency, the higher the value of f, the more the current density will be focused closer to the surface (skin effect), which reflects a shielding barrier effect for external magnetic fields.

The above-discussed physical occurrences dictate EMF behaviors including EM radiation and stray fields and their adverse effects on exposed matters. The articulation of the link between such theoretical approach and practical applications will be illustrated in Section 5.

2.1. Evaluation of EMF expected outcomes and side effects

The EMFs Maxwell equations function of the 3D vector variables **H, E, B, D,** and **J** and the material parameters μ, ε, and σ as well as the operational frequency f permit for given source field value and topological features of the concerned device, to obtain the different induced fields in matter and airgap (outside matter) space fields. The induced matter fields allow the determination of global quantiles as forces, dissipated losses, etc.

Such quantities can be used in EM energy conversion devices, associated with the conversion energy form, equation to determine the expected outcome or the side effect. For example, the EM forces permit associated with mechanical equation the calculation of expected torque and unwanted vibrations. As well, dissipated EM energy enable associated with heat transfer (HT) equation to obtain the expected temperature rise in heating systems and unsolicited heating. In addition, the obtained space fields permit the determination of expected power transfer (in transmission systems) as well as stray or radiated fields.

2.2. Evaluation of adverse effects due to stray or radiated fields

The evaluation and control of different adverse effects involving perturbation of medical tools or biological effects (BEs) in living tissues in general require the solution of EMF equations with HT or bio-heat (BH) equations according to the corresponding situation. Actually, the paper analyzes the physical effects of EMF. When these effects present threat or harm to human or more generally biodiversity and ecosystem, the goal is to investigate the evaluation, control via standard safety guidelines, and protection from these effects.

3. Governing Equations

Concerning the projected effects and adverse effects of EMFs on living tissues and health devices, the involved governing equations are the object of this section.

Based on the Maxwell's microscopic local comportment, the differential structure of the general EMF 4 equations [26] and the general HT equation in its differential formulation are given by:

$$\nabla \times \mathbf{E} = -\partial_t \mathbf{B}\,(\text{Maxwell} - \text{Faraday}) \tag{1}$$

$$\nabla \times \mathbf{H} = \sigma \mathbf{E} + \partial_t \mathbf{D}\,(\text{Maxwell} - \text{Ampere}) \tag{2}$$

$$\nabla \cdot \mathbf{D} = \rho_e\,(\text{Maxwell} - \text{Gauss}) \tag{3}$$

$$\nabla \cdot \mathbf{B} = 0\,(\text{Maxwell} - \text{Thomson}) \tag{4}$$

The HT equation in its differential formulation is given by:

$$\mathrm{c}\,\rho\,\partial \mathrm{T}/\partial \mathrm{t} = \nabla \cdot (\mathrm{k} \nabla \mathrm{T}) \tag{5}$$

In the case of EMF radiation of living tissues or objects in general, the equations of the EMF harmonic fields, of BH and of its heat source P_{d}, corresponding to the dissipated EM energy allowing the EMF-BH coupling are given as follows:

$$\nabla \times \mathbf{H} = \mathbf{J} \tag{6}$$

$$\mathbf{J} = \mathbf{J_e} + \sigma \mathbf{E} + j\omega \mathbf{D} \tag{7}$$

$$\mathbf{E} = -\nabla V - j\omega \mathbf{A} \tag{8}$$

$$\mathbf{B} = \nabla \times \mathbf{A} \tag{9}$$

$$\mathrm{c}\,\rho\,\partial \mathrm{T}/\partial \mathrm{t} = \nabla \cdot (\mathrm{k} \nabla \mathrm{T}) + \mathrm{P_d} + \mathrm{P_t} + \mathrm{c_f}\rho_{\mathrm{f}}\mathrm{p_f}(\mathrm{T_f} - \mathrm{T}) \tag{10}$$

$$\mathrm{P_d} = \omega \cdot \varepsilon'' \cdot \mathrm{E}^2/2 \tag{11}$$

In Equations (1)–(11), the previously defined symbols are the vectors **H, E, B, D,** and **J** as well as the parameters μ, ε, and σ besides the operational frequency f. In addition, **A** and V are the magnetic vector and electric scalar potentials in Wb/m and volt. $\mathbf{J_e}$ is the vector of the source current density in A/m^2, ρ_{e} is the volume density of electric

charges in C/m^3. The symbol ∇ is a vector of partial derivative operators. The symbol ∂_t is the operator of partial time derivative. The parameters ε'' is the imaginary part of the complex permittivity of the absorbing material and ρ is the material density in kg/m^3. E is the absolute peak value of the electric field strength in V/m, c is the specific heat of the substance in J/(kg °C), k is thermal conductivity in W/(m• °C), and T is the substance temperature in °C. The power dissipation in W/m^3 given by Equation (11) relates to principal dielectric heating of EMF energy loss. Notice that the imaginary part ε'' of the (frequency-dependent) ε denotes an ability scale of a dielectric to convert EMF energy into heat. The power dissipation volume density given by Equation (11) will be used in the coupling of EMF and BH equations. In the case of living tissues, Equation (10) includes a term of self-tissue heat source P_t, a term of external heat source related to the EMF exposure P_d, and a term of convective heat transfer via irrigating fluid of tissue. P_t and P_d are heat sources in W/m^3, T_f and T are respectively the fluid temperature and the local temperature of tissue in °C, and c_f, ρ_f, p_f are respectively fluid, specific heat in J/(kg °C), density in kg/m^3, perfusion rate in 1/s.

Note that the source term in Equation (7) is the source current density $\mathbf{J_e} = \sigma\, \mathbf{E_e}$. In addition, the specific absorption rate (SAR) in biological tissues is equal to P_d/ρ in W/kg. In addition, Equation (10) corresponds to bio-heat living tissues allowing for the EMF exposure. Such representation is comparable to the Penne's bio-heat equation [14, 27, 28] linked to living tissues of human and animal including blood convective heat transfer. Equation (10) is generalized to biodiversity tissues. The plant sap fluid plays the role of blood and Phloem and Xylem walling sap accomplish the duty of veins and arteries confining blood. The term P_t in Equation (10) is related to animal metabolic heat or to internal heat in plant tissues. In addition, the last term in Equation (10) relative to convection heat transfer in fluid relates to human-animal blood or plant sap.

3.1. EMF Source and target living tissues or medical tools

EM devices in general, as mentioned before, are energy conversion or transfer devices, characterized by expected and undesired actions. In these situations, an EM device includes both actions. Regarding their side effect action, these devices could act as a source for nearby materials or tools. These would be disturbed due to exposure to the side effects of EM devices. The stray fields of these will disturb the operation and heat these nearby objects due to the energy dissipated by EM radiation added to the heat conduction and convection caused by the thermal side effect of EM devices.

In the case of radiating EM devices, the geometric structure involved in the mathematical model is that of the EM device for the determination of expected actions and side effects for energy conversion and transfer devices. The source term corresponds to the input voltage or current of the device. The concerned equations in this task are those of Equations (6)–(9).

In the case of target objects for EM exposure such as living tissues or medical tools, the geometry concerned corresponds to these objects and the source term relates to the radiation field of the exponent or the heat source, both resulting from the side effects of EM devices. The solution of Equations (6)–(11) permits the evaluation of the different induced fields in living tissues or medical tools.

Due to the geometrical complexity and non-linear behavior of modeled entities (radiating source device, radiated tissue, or medical tool), local solution specifying the practice of discretized 3D methods as finite elements or equivalent methods [29–35] associated with appropriate coupling strategies of equations [36].

3.2. RA and OH approaches in device design

The RA and OH approaches permit, through Eco-design, enhancing expected outcome and reducing side effects of radiating EM devices as well as protecting the exposed tools. Thus, such Eco-design includes optimization of device construction as well as its protection [37] as discussed in Sections 4 and 5. These tools, in addition to their reduced radiation, could be constructed of EMF-insensitive matters or shielded. Figure 1 [37] summarizes the role of the RA and OH in the management of EMF exposure of an onboard tool [37].

4. Protection Against EMF Exposure

EM interference (EMI), which contains various unwanted emitted signals, can be checked by EM compatibility (EMC) analysis. Shielding equipment generally uses substances that absorb or redirect the radiated electromagnetic wave to inhibit its

Figure 1
RA and OH approaches involving the Eco-design and use of onboard tool considering urban biodiversity via handling of adverse EMF effects

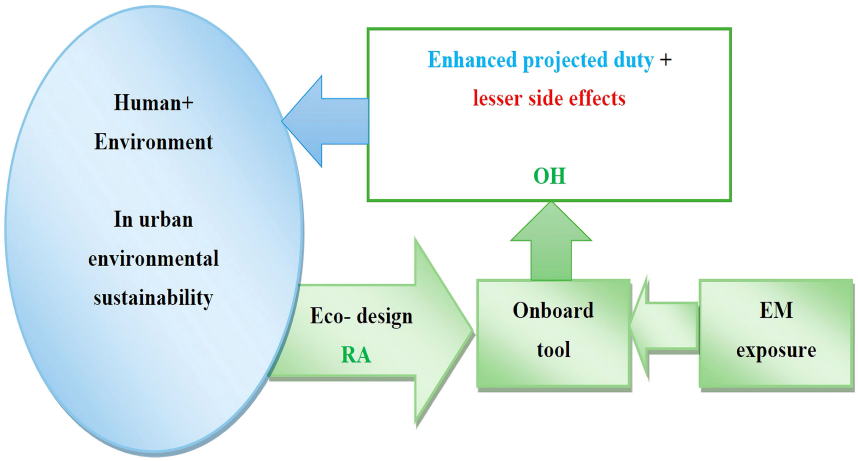

path between the two sides of the shielding layer. EMI shielding, which retains EMF radiation, is essential for protecting human health and devices. An EMF generally involves **H** and **E** fields directed perpendicularly in space. Thus, EMI shielding schemes are classified into magnetic, electric, and coupled EMI shielding. In addition, the high-frequency waves that characterize radiation contain interdependent **H** and **E** fields. Therefore, shielding one of the two fields would result in the reduction of the other. Therefore, EMI shields are generally made of conductive substances for simplicity. The type of shielding material is related to the application concerned, it can be clothing, rubbers, adhesives, or coatings. These are related to the required flexibility, fixing capacity, ease of processing, and consistency, their worth could be found, e.g., in references [38–46].

4.1. Smart shielding strategies

As mentioned above, shields made of conductive material have the advantage of simplicity. However, such simple shields would involve heating of their material due to internal induced currents. Such heating would increase the temperature of the adjacent shielded device or the living tissues in contact with it. If such a temperature increase is intolerable, we are forced to adapt the conductive nature of the shield. In fact, two basic types of losses, reflection and absorption losses support the shielding against electromagnetic radiation. In the case of conductive shielding, the surface electrical impedance function of the EM parameters is $Z_s = (\omega \cdot \mu/\sigma)^{1/2}$. Such impedance is greatly inferior to the impedance of free space $Z_0 = (\mu_0/\varepsilon_0)^{1/2} \approx 376.7$ ohm. When a plane wave field strikes a shielding layer, the encountered high impedance difference generates large reflections. The remaining field is sent through the layer after partial absorption. A high-frequency radiated field would only penetrate the near-surface edge of a conductor, due to the last-mentioned skin effect. The associated skin depth is given by $\delta = (\omega \cdot \mu \cdot \sigma/2)^{-1/2}$. Note that this formula is only valid for δ greater than the electron mean free path in the substance. Regarding reflection and absorption losses, the former decreases with frequency while the latter, which is related to the thickness of the shielding layer, increases with frequency. Together, the two losses denote the total shielding effectiveness (SE), which is labeled as the ratio of EMFs without and with the shielded device. Thus, the abovementioned adaptation of the conductive nature of the shielding could be achieved by the use of multifunctional materials suitable for low-reflectivity EMI shielding. Such material customization can reduce the strong reflection due to the high conductivity of the material. Moreover, a particular manufacturing process can decrease the reflected power coefficient of the material, added to losses reduction, improved thermal protection and environmentally friendly shielding materials, can be very effective. Quantitative assessments of their effectiveness could be found, e.g., in references [47–53]. The control of SE could be realized with the solution of Equations (6)–(9).

5. Examples of Adverse Effects of EMF Exposures

In this section, we consider the cases of evaluation and management (control of device integrity or BEs) of the adverse EMF effects on health devices and living tissues illustrated through two applications. The first is related to the case of EMC analysis for the control of the integrity of the RF field involved in an MRI due to the introduction of external EMF-sensitive matter in the imager. The second concerns the case of safety control of an EMF exposure of an IPT via its inductive coupler transformer (ICT) on living tissues of a human body. The numerical technique used in both applications is finite element method, the practical details, and accuracy of the method are demonstrated in references [29–36]. These cases considered in these two examples are among others, e.g., exposure of different types of 5G communication devices on surrounding biological tissues under long-term low-intensity exposure, EMF exposure impact for emerging wearable medical devices such as implantable heart monitors, etc.

5.1. EMC control of the integrity of the MRI RF-EMF

Disturbances in the image-related RF magnetic field distribution inside an MRI tunnel are typically triggered by external electromagnetic fields or by the introduction of magnetic or conductive substances into the imager environment. In MRI-assisted therapies and interventions, only actuation devices constructed from non-magnetic and non-conductive constituents such as piezoelectric materials are allowed. Piezoelectric actuators [54–58] use thin conductive electrodes for their excitation. The orientation of these thin electrodes with respect to the field plays an important role related to the weight of the conductive surface perpendicular to the field direction; thus, the higher this weight, the higher the corresponding disturbance will be. This phenomenon, which is related to induced eddy currents, could be used in the context of actuation to reduce disorder in the RF field distribution [7].

Figure 2 [27] shows, at 63.87 MHz (for static magnetic field B_0 of 1.5 T), the MRI RF magnetic field distribution (vertically directed) in the birdcage axial section inside the tunnel of MRI for the no-material case. Figure 3 [27] shows the case of a cubic piezoelectric with relative permeability and permittivity, and

Figure 2
MRI RF (at 63.87 MHz, B_0 1.5 T) magnetic field (vertically directed) distribution in the case of no material in the birdcage inside the MRI tunnel

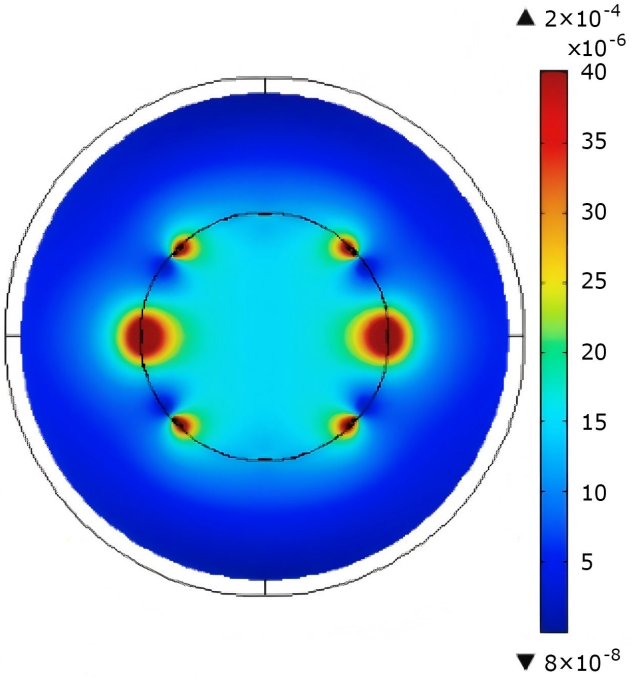

Figure 3
MRI RF magnetic field distribution with the insertion of a piezoelectric coated by electrodes: (a) material outline, (b) field distribution with electrodes perpendicular to the field, and (c) field distribution with electrodes parallel to the field

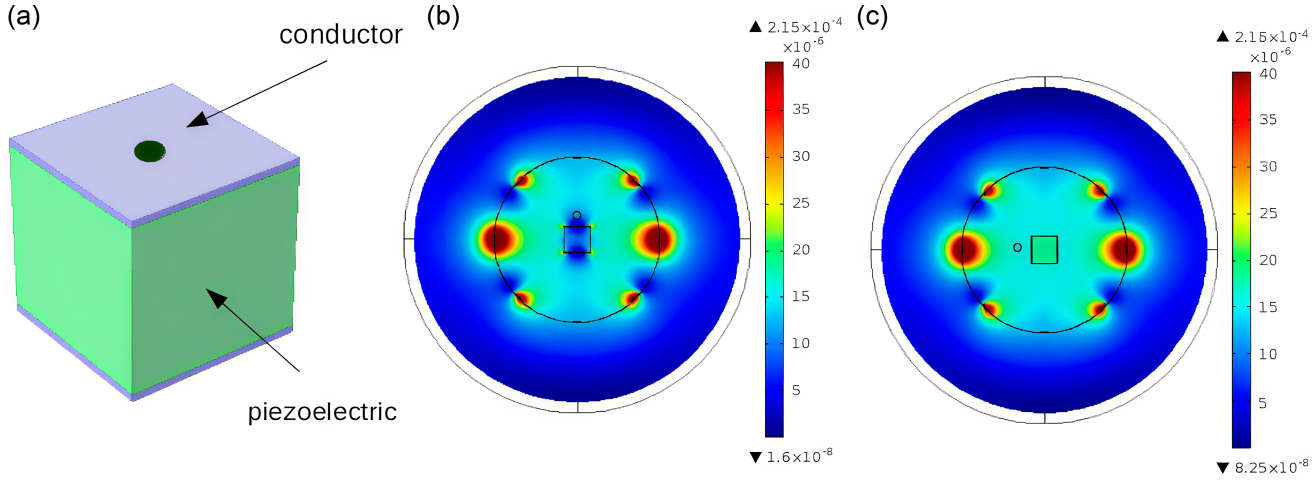

conductivity of ($\mu_r = 1$, $\varepsilon_r = [450,990,990]$, $\sigma = 0$ S/m) covered on two opposite faces by thin electrodes with ($\mu_r = 1$, $\varepsilon_r = 1$, $\sigma = 3.77 \times 10^7$ S/m) (see Figure 3(a)). In addition, Figure 3(b) and (c) show respectively the field distributions in the two situations where the electrodes are perpendicular and parallel to the field direction. In the last case, the effect of the conductors (parallel to the field) is significantly reduced (see Figures 2 and 3(c)).

This example of MRI EMC monitoring illustrates an analysis, control, and design policy related to possible disorders and their treatment in image-assisted interventions or integrated therapies.

5.2. Control of IPT exposure BEs in living tissues

An example of ICT EMF radiation demonstration on living tissues of a human body placed horizontally on the ground alongside an EV during static charging of its batteries is presented in this section [27]. The ICT and its connected circuits were designed and controlled to

Figure 4
Activated field distributions in a body exposed to an ICT (3kW, 30 kHz) under an EV, for a horizontal ground placed body beside the EV. (a) B (T), (b) E (V/m)

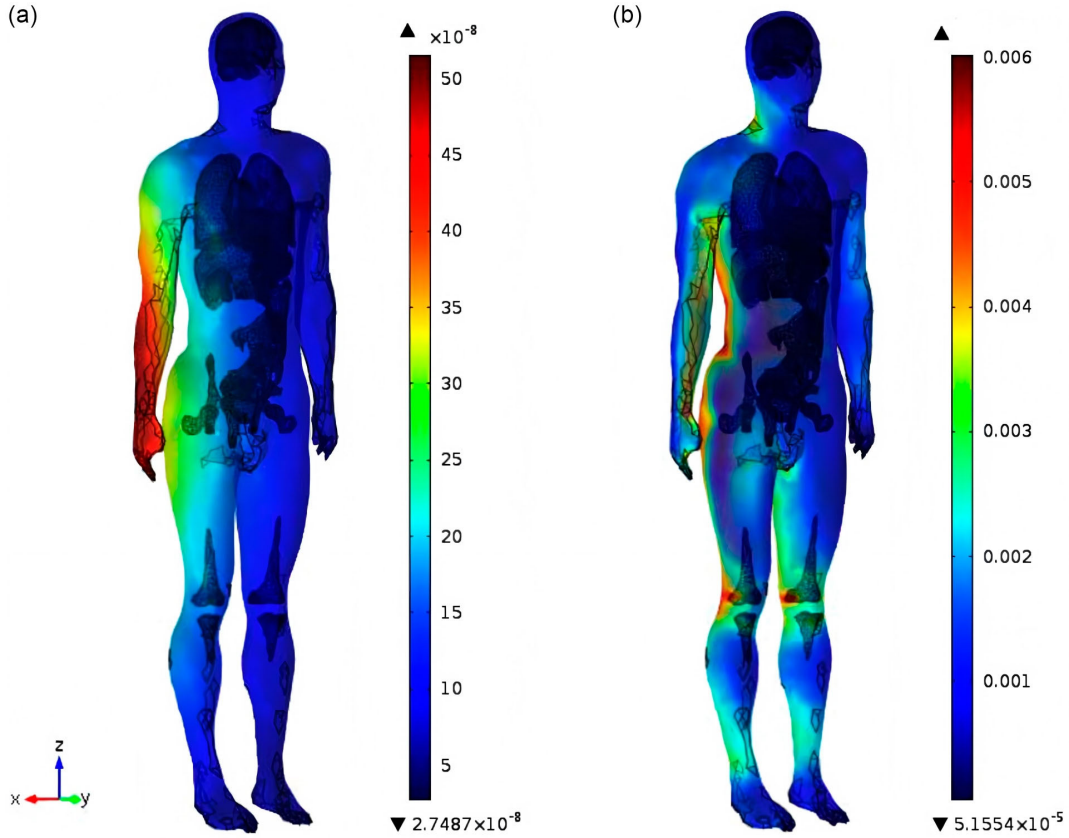

maximize the transferred power and minimize stray fields. Figure 4 [27] presents the distributions of the induced fields in the body (B and E) due to exposure to ICT stray fields. A high-resolution human anatomical model was used, compatible with the numerical approach used, in these calculations. The results obtained in such a case were compared to thresholds fixed by regulations and found to be within standard safety guidelines (27 μT for magnetic induction B and 4.05 V/m for electric field E) [59, 60].

6. Discussion

Following the analyses in the previous sections, several topics deserve to be discussed in more detail:

Electromagnetic disturbances or noise in a device can be due to radiation from an external source or to the presence or insertion of materials sensitive to EMFs in the device. In fact, there are three categories of devices. Those that have their own EMF in their operation, those without fields but containing materials sensitive to EMFs, and finally those without fields or materials sensitive to EMFs. The latter are not disturbed by external fields. The second must be shielded. In the first case, the effects of external fields and/or the insertion of materials sensitive to EMFs must be circumvented.

Regarding shielding, a source and a target characterize an EMF exposure. A shield placed between the two could ensure the protection of the target from the source. Such a shield could be placed anywhere along the entire distance between the sides of the source and the target. However, this is not always possible. For example, in protecting people or animals inside an EV from the ICT placed under the vehicle, the shielding would be easy, while for those outside close to the vehicle, it is more complicated or even impossible, due to the structure of the ICT (one coil under the vehicle bottom separated from the other on the ground). Another issue is the placement of the shield on the source or target. If the shield is on the source device, it can prevent the device from working. If the shield is on the target, it should not be simply conductive but a more expensive smart shield to prevent the target from heating up due to dissipation in the conductor.

Exposure to EMFs of sufficient magnitude (intensity and duration) can be harmful to living organisms. Generally, the interaction of EMFs with a matter because of field exposure triggers a dissipation of EM energy in the matter. Different effects are initiated in living tissues due to this dissipation, generally correlated with the strength and frequency of the EMF. Such exposure can lead to heating of living tissues, causing an increase in temperature, which can initiate tissue damage. Such thermal BEs due to EMF exposure include tissues of human, fauna, and flora. Two factors aggravate this phenomenon. The first is related to the ability of high-frequency energy to rapidly heat biological tissues. The second is related to the inability of tissues to tolerate or dissipate the heat that can be created. In addition, the parts of tissues least protected from heating by EMFs are those that lack available fluid circulation (blood or sap), which is the primary mode of coping with intense heat. The extent of this heating is related to a number of factors, including field strength, frequency, duration of exposure, heat dissipation capacity of the tissues, surrounding environment, and the size, shape, and location of the exposed tissue. In fact, typical thermal BEs on tissues usually occur in cases of reduced radiation due to normal shielding, short exposure time, and long distance from the source. In contrast, living tissues irradiated at disproportionate SAR values, field strengths, frequencies, or time intervals can lead to non-thermal effects and undergo unalterable molecular disturbances that can stimulate nerves, muscles, and generally excitable organisms. One of the most common effects in this context is the disruption of brain electrical waves due to altered cellular secretion. Also, EM-induced membrane electroporation can disrupt cellular activation as well. Figure 5 illustrates a summary diagram of onboard device control strategies and EMF exposure behaviors.

Figure 5
Summary illustration of onboard device control strategies and EMF exposure behaviors

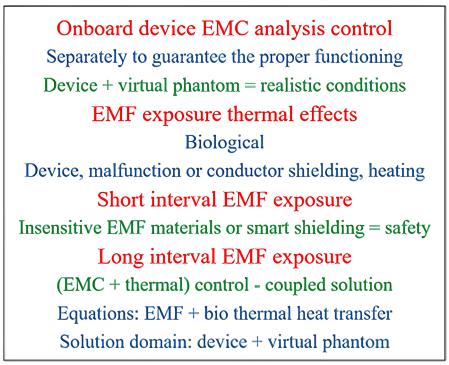

The practice of RA and OH approaches allows for better sustainable device performance, enhanced well-being of biodiversity, and protected Eco-system. Moreover, in all device circumstances, a prognostic check could be experienced by means of EMC control counting disturbs, design, shielding, etc., thus adopting the roles of RA and OH approaches.

The different models used in this contribution may involve uncertainty and hence need error estimation and possible experimental validation. Such uncertainty could be treated through management of procedures control via matching digital twins allowing for physical and model uncertainty reduction [61–67].

7. Conclusions

In this contribution, the assessment of risk and protection against the adverse effects of EMF on living tissues and near-tissues health devices has been carried out. The results of the investigation illustrate that the physical events involved in the origins of radiation and stray fields, as well as their adverse effects on exposed materials and their protection, allow a thorough understanding and control of their management. Moreover, the corresponding mathematical formulations dictating the behaviors of the involved EMFs allow their assessment by 3D local calculations according to RA and OH approaches that enable ecological biodiversity and the ecosystem. Future research prospects could be the management of procedures control via matching digital twins allowing for physical and model uncertainties treatments.

Conflicts of Interest

The author declares that he has no conflicts of interest to this work.

Data Availability Statement

Data sharing is not applicable to this article as no new data were created or analyzed in this study.

Author Contribution Statement

Adel Razek: Conceptualization, Methodology, Software, Validation, Formal analysis, Investigation, Resources, Data

Curation, Writing – original draft, Writing – review & editing, Visualization, Supervision, Project administration.

References

[1] Mackenzie, J. S., & Jeggo, M. (2019). The One Health approach—Why is it so important? *Tropical Medicine and Infectious Disease*, *4*(2), 88. https://doi.org/10.3390/tropicalmed4020088

[2] Deiana, G., Arghittu, A., Dettori, M., & Castiglia, P. (2024). One world, One Health: Zoonotic diseases, parasitic diseases, and infectious diseases. *Healthcare*, *12*(9), 922. https://doi.org/10.3390/healthcare12090922

[3] Chakrabarti, S., Biswas, N., Jones, L. D., Kesari, S., & Ashili, S. (2022). Smart consumer wearables as digital diagnostic tools: A review. *Diagnostics*, *12*(9), 2110. https://doi.org/10.3390/diagnostics12092110

[4] Escobar-Linero, E., Muñoz-Saavedra, L., Luna-Perejón, F., Sevillano, J. L., & Domínguez-Morales, M. (2023). Wearable health devices for diagnosis support: Evolution and future tendencies. *Sensors*, *23*(3), 1678. https://doi.org/10.3390/s23031678

[5] Devi, D. H., Duraisamy, K., Armghan, A., Alsharari, M., Aliqab, K., Sorathiya, V., . . . , & Rashid, N. (2023). 5G technology in healthcare and wearable devices: A review. *Sensors*, *23*(5), 2519. https://doi.org/10.3390/s23052519

[6] Moon, K. S., & Lee, S. Q. (2023). A wearable multimodal wireless sensing system for respiratory monitoring and analysis. *Sensors*, *23*(15), 6790. https://doi.org/10.3390/s23156790

[7] Germann, C., Nanz, D., & Sutter, R. (2021). Magnetic resonance imaging around metal at 1.5 Tesla: techniques from basic to advanced and clinical impact. *Investigative Radiology*, *56*(11), 734–748. https://doi.org/10.1097/RLI.0000000000000798

[8] Rendón Vélez, S., van Helvoort, M. J. A. M., Vogt-Ardatjew, R., van den Berg, B., & Leferink, F. (2023). Challenges in risk-based EMC for MRI systems. In *2023 International Symposium on Electromagnetic Compatibility – EMC Europe*, 1–6. https://doi.org/10.1109/EMCEurope57790.2023.10274190

[9] Khan Mamun, M. M. R., & Sherif, A. (2023). Advancement in the cuffless and noninvasive measurement of blood pressure: A review of the literature and open challenges. *Bioengineering*, *10*(1), 27. https://doi.org/10.3390/bioengineering10010027

[10] Bhuva, A. N., Moralee, R., Brunker, T., Lascelles, K., Cash, L., Patel, K. P., . . . , & Manisty, C. H. (2022). Evidence to support magnetic resonance conditional labelling of all pacemaker and defibrillator leads in patients with cardiac implantable electronic devices. *European Heart Journal*, *43*(26), 2469–2478. https://doi.org/10.1093/eurheartj/ehab350

[11] Joo, H., Lee, Y., Kim, J., Yoo, J. S., Yoo, S., Kim, S., . . . , & Kim, D. H. (2021). Soft implantable drug delivery device integrated wirelessly with wearable devices to treat fatal seizures. *Science Advances*, *7*(1), eabd4639. https://doi.org/10.1126/sciadv.abd4639

[12] Cheng, Y., Xie, D., Han, Y., Guo, S., Sun, Z., Jing, L., . . . , & Lu, Y. (2023). Precise management system for chronic intractable pain patients implanted with spinal cord stimulation based on a remote programming platform: Study protocol for a randomized controlled trial (PreMaSy study). *Trials*, *24*(1), 580. https://doi.org/10.1186/s13063-023-07595-4

[13] Su, H., Kwok, K. W., Cleary, K., Iordachita, I., Cavusoglu, M. C., Desai, J. P., & Fischer, G. S. (2022). State of the art and future opportunities in MRI-guided robot-assisted surgery and interventions. *Proceedings of the IEEE*, 110(7), 968–992. https://doi.org/10.1109/JPROC.2022.3169146

[14] Singh, S., Torrealdea, F., & Bandula, S. (2021). MR imaging–guided intervention: Evaluation of MR conditional biopsy and ablation needle tip artifacts at 3T using a balanced fast field echo sequence. *Journal of Vascular and Interventional Radiology*, *32*(7), 1068–1074. https://doi.org/10.1016/j.jvir.2021.03.536

[15] Miclaus, S., Deaconescu, D. B., Vatamanu, D., & Buda, A. M. (2023). An exposimetric electromagnetic comparison of mobile phone emissions: 5G versus 4G signals analyses by means of statistics and convolutional neural networks classification. *Technologies*, *11*(5), 113. https://doi.org/10.3390/technologies11050113

[16] Miclaus, S., Deaconescu, D. B., Vatamanu, D., & Buda, A. M. (2024). Mobile phone emissions in 5G FR1: Using statistic inferences and deep learning for empiric features extraction. In *2024 IEEE International Symposium on Measurements & Networking*, 01–06. https://doi.org/10.1109/MN60932.2024.10615263

[17] Karipidis, K., Baaken, D., Loney, T., Blettner, M., Brzozek, C., Elwood, M., . . . , & Lagorio, S. (2024). The effect of exposure to radiofrequency fields on cancer risk in the general and working population: A systematic review of human observational studies – Part I: Most researched outcomes. *Environment International*, *191*, 108983. https://doi.org/10.1016/j.envint.2024.108983

[18] Chikha, W. B., Zhang, Y., Liu, J., Wang, S., Sandeep, S., Guxens, M., . . . , & Wiart, J. (2024). Assessment of radio frequency electromagnetic field exposure induced by base stations in several micro-environments in France. *IEEE Access*, *12*, 21610–21620. https://doi.org/10.1109/ACCESS.2024.3363914

[19] Sivani, S., & Sudarsanam, D. (2012). Impacts of radio-frequency electromagnetic field (RF-EMF) from cell phone towers and wireless devices on biosystem and ecosystem—A review. *Biology and Medicine*, *4*(4), 202–216.

[20] Shah, I. A., Zada, M., Shah, S. A. A., Basir, A., & Yoo, H. (2024). Flexible metasurface-coupled efficient wireless power transfer system for implantable devices. *IEEE Transactions on Microwave Theory and Techniques*, *72*(4), 2534–2547. https://doi.org/10.1109/TMTT.2023.3319050

[21] Kod, M., Zhou, J., Huang, Y., Hussein, M., Sohrab, A. P., & Song, C. (2021). An approach to improve the misalignment and wireless power transfer into biomedical implants using meandered wearable loop antenna. *Wireless Power Transfer*, *8*(1), 6621899. https://doi.org/10.1155/2021/6621899

[22] Zhou, J., Guo, K., Chen, Z., Sun, H., & Hu, S. (2020). Design considerations for contact-less underwater power delivery: A systematic review and critical analysis. *Wireless Power Transfer*, *7*(1), 76–85. https://doi.org/10.1017/wpt.2020.3

[23] Wu, J., Li, Y., Dai, X., Gao, R., & He, M. (2024). A dynamic power transfer route construction and optimization method considering random node distribution for wireless power transfer network. *IEEE Transactions on Power Electronics*, *39*(4), 4858–4869. https://doi.org/10.1109/TPEL.2023.3348103

[24] Razek, A. (2024). Sustainable wireless power transfer in the context of One Health environmental approach. *Wireless Power Transfer*, *11*(1), e003. https://doi.org/10.48130/wpt-0024-0003

[25] Razek, A. (2024). Interaction of electromagnetic fields with body-onboard devices. *Exploration of Digital Health Technologies*, *2*(3), 124–134. https://doi.org/10.37349/edht.2024.00015

[26] Maxwell, J. C. (1865). A dynamical theory of the electromagnetic field. *Philosophical Transactions of the Royal Society of London*, *155*, 459–512. https://doi.org/10.1098/rstl.1865.0008

[27] Razek, A. (2022). Biological and medical disturbances due to exposure to fields emitted by electromagnetic energy devices —A review. *Energies*, *15*(12), 4455. https://doi.org/10.3390/en15124455

[28] Pennes, H. H. (1948). Analysis of tissue and arterial blood temperatures in the resting human forearm. *Journal of Applied Physiology*, *1*(2), 93–122. https://doi.org/10.1152/jappl.1948.1.2.93

[29] Antunes, O. J., Bastos, J. P. A., Sadowski, N., Razek, A., Santandrea, L., Bouillault, F., & Rapetti, F. (2005). Using hierarchic interpolation with mortar element method for electrical machines analysis. *IEEE Transactions on Magnetics*, *41*(5), 1472–1475. https://doi.org/10.1109/TMAG.2005.844561

[30] Cicuttin, M., & Geuzaine, C. (2024). Numerical investigation of a 3D hybrid high-order method for the indefinite time-harmonic Maxwell problem. *Finite Elements in Analysis and Design*, *233*, 104124. https://doi.org/10.1016/j.finel.2024.104124

[31] Seebacher, P., Kaltenbacher, M., Wein, F., & Lehmann, H. (2021). A pseudo density topology optimization approach in nonlinear electromagnetism applied to a 3D actuator. *International Journal of Applied Electromagnetics and Mechanics*, *65*(3), 545–559. https://doi.org/10.3233/JAE-201501

[32] Urdaneta-Calzadilla, A., Galopin, N., Niyonzima, I., Chadebec, O., Meunier, G., & Bannwarth, B. (2024). FEM-BEM modeling of nonlinear magnetoelectric effects in heterogeneous composite structures. *IEEE Transactions on Magnetics*, *60*(3), 1–4. https://doi.org/10.1109/TMAG.2023.3339088

[33] Song, W., Han, Y., Yang, F., Pang, J., Wang, L., Cao, J., & Deng, S. (2024). Magnetostrictive vibration characteristics of amorphous alloy transformer with three-dimensional wound core. *IEEE Access*, *12*, 43958–43967. https://doi.org/10.1109/ACCESS.2024.3380456

[34] Wang, S. J., & Zhao, Q. (2024). A lowest-order mixed mortar-element method for 3-D Maxwell's eigenvalue problems with the absorbing boundary condition. *IEEE Transactions on Microwave Theory and Techniques*, *72*(7), 3970–3979. https://doi.org/10.1109/TMTT.2023.3342030

[35] Qin, Z., Talleb, H., & Ren, Z. (2016). A proper generalized decomposition-based solver for nonlinear magnetothermal problems. *IEEE Transactions on Magnetics*, *52*(2), 1–9. https://doi.org/10.1109/TMAG.2015.2492462

[36] Gu, B., Li, H., & Li, B. (2024). An internal ballistic model of electromagnetic railgun based on PFN coupled with multi-physical field and experimental validation. *Defence Technology*, *32*, 254–261. https://doi.org/10.1016/j.dt.2023.08.015.

[37] Razek, A. (2024). Sustainable design and integrity control of onboard health tools for humans and their environmental urban biodiversity. *Intelligent and Sustainable Manufacturing*, *1*(2), 10015. https://doi.org/10.70322/ism.2024.10015

[38] Chen, C. H., Huang, C. Y., & Huang, Y. C. (2022). Improving the electromagnetic compatibility of electronic products by using response surface methodology and artificial neural network. *Microelectronics International*, *39*(1), 1–13. https://doi.org/10.1108/MI-06-2021-0052

[39] Yang, Y., Zeng, S., Li, X., Hu, Z., & Zheng, J. (2022). Ultrahigh and tunable electromagnetic interference shielding performance of PVDF composite induced by nano-micro cellular structure. *Polymers*, *14*(2), 234. https://doi.org/10.3390/polym14020234

[40] Yao, B., Hong, W., Chen, T., Han, Z., Xu, X., Hu, R., . . . , & Wang, H. (2020). Highly stretchable polymer composite with strain-enhanced electromagnetic interference shielding effectiveness. *Advanced Materials*, *32*(14), 1907499. https://doi.org/10.1002/adma.201907499

[41] Yun, T., Kim, H., Iqbal, A., Cho, Y. S., Lee, G. S., Kim, M., . . . , & Koo, C. M. (2020). Electromagnetic shielding of monolayer MXene assemblies. *Advanced Materials*, *32*(9), 1906769. https://doi.org/10.1002/adma.201906769

[42] Song, W. L., Cao, M. S., Lu, M. M., Bi, S., Wang, C. Y., Liu, J., . . . , & Fan, L. Z. (2014). Flexible graphene/polymer composite films in sandwich structures for effective electromagnetic interference shielding. *Carbon*, *66*, 67–76. https://doi.org/10.1016/j.carbon.2013.08.043

[43] Song, W. L., Guan, X. T., Fan, L. Z., Cao, W. Q., Wang, C. Y., & Cao, M. S. (2015). Tuning three-dimensional textures with graphene aerogels for ultra-light flexible graphene/texture composites of effective electromagnetic shielding. *Carbon*, *93*, 151–160. https://doi.org/10.1016/j.carbon.2015.05.033

[44] Tan, Y. J., Li, J., Gao, Y., Li, J., Guo, S., & Wang, M. (2018). A facile approach to fabricating silver-coated cotton fiber non-woven fabrics for ultrahigh electromagnetic interference shielding. *Applied Surface Science*, *458*, 236–244. https://doi.org/10.1016/j.apsusc.2018.07.107

[45] Han, M., Yin, X., Hantanasirisakul, K., Li, X., Iqbal, A., Hatter, C. B., . . . , & Gogotsi, Y. (2019). Anisotropic MXene aerogels with a mechanically tunable ratio of electromagnetic wave reflection to absorption. *Advanced Optical Materials*, *7*(10), 1900267. https://doi.org/10.1002/adom.201900267

[46] Mohammad, M., Wodajo, E. T., Choi, S., & Elbuluk, M. E. (2019). Modeling and design of passive shield to limit EMF emission and to minimize shield loss in unipolar wireless charging system for EV. *IEEE Transactions on Power Electronics*, *34*(12), 12235–12245. https://doi.org/10.1109/TPEL.2019.2903788

[47] Quercio, M., Lozito, G. M., Corti, F., Riganti Fulginei, F., & Laudani, A. (2024). Recent results in shielding technologies for wireless electric vehicle charging systems. *IEEE Access*, *12*, 16728–16740. https://doi.org/10.1109/ACCESS.2024.3357526

[48] Cheng, J., Li, C., Xiong, Y., Zhang, H., Raza, H., Ullah, S., . . . , & Che, R. (2022). Recent advances in design strategies and multifunctionality of flexible electromagnetic interference shielding materials. *Nano-Micro Letters*, *14*(1), 80. https://doi.org/10.1007/s40820-022-00823-7

[49] Ma, Z., Deng, Z., Zhou, X., Li, L., Jiao, C., Ma, H., . . . , & Zhang, H. B. (2023). Multifunctional and magnetic MXene composite aerogels for electromagnetic interference shielding with low reflectivity. *Carbon*, *213*, 118260. https://doi.org/10.1016/j.carbon.2023.118260

[50] Yun, J., Zhou, C., Guo, B., Wang, F., Zhou, Y., Ma, Z., & Qin, J. (2023). Mechanically strong and multifunctional nano-nickel aerogels based epoxy composites for ultra-high electromagnetic interference shielding and thermal management. *Journal of Materials Research and Technology*, *24*, 9644–9656. https://doi.org/10.1016/j.jmrt.2023.05.193

[51] Verma, R., Thakur, P., Chauhan, A., Jasrotia, R., & Thakur, A. (2023). A review on MXene and its' composites for electromagnetic interference (EMI) shielding applications. *Carbon*, *208*, 170–190. https://doi.org/10.1016/j.carbon.2023.03.050

[52] Kostishin, V. G., Isaev, I. M., & Salogub, D. V. (2024). Radio-absorbing magnetic polymer composites based on spinel ferrites: A review. *Polymers*, *16*(7), 1003. https://doi.org/10.3390/polym16071003

[53] Zecchi, S., Cristoforo, G., Bartoli, M., Tagliaferro, A., Torsello, D., Rosso, C., . . . , & Acerra, F. (2024). A comprehensive

review of electromagnetic interference shielding composite materials. *Micromachines*, *15*(2), 187. https://doi.org/10.3390/mi15020187

[54] Lemaire, E., Moser, R., Borsa, C. J., Shea, H., & Briand, D. (2015). Green paper-based piezoelectric material for sensors and actuators. *Procedia Engineering*, *120*, 360–363. https://doi.org/10.1016/j.proeng.2015.08.637

[55] Liu, J., Ding, Z., Wu, J., Wang, L., Chen, T., Rong, X., . . . , & Li, Y. (2025). A self-moving piezoelectric actuator with high carrying/positioning capability via bending-resonant-vibration-induced stick-slip motion. *IEEE Transactions on Industrial Electronics*, *72*(2), 1829–1839. https://doi.org/10.1109/TIE.2024.3429612

[56] Dagdeviren, C., Joe, P., Tuzman, O. L., Park, K. I., Lee, K. J., Shi, Y., . . . , & Rogers, J. A. (2016). Recent progress in flexible and stretchable piezoelectric devices for mechanical energy harvesting, sensing and actuation. *Extreme Mechanics Letters*, *9*, 269–281. https://doi.org/10.1016/j.eml.2016.05.015

[57] Stapleton, A., Noor, M. R., Sweeney, J., Casey, V., Kholkin, A. L., Silien, C., . . . , & Tofail, S. A. M. (2017). The direct piezoelectric effect in the globular protein lysozyme. *Applied Physics Letters*, *111*(14), 142902. https://doi.org/10.1063/1.4997446

[58] Su, Q., Quan, Q., Deng, J., & Yu, H. (2018). A quadruped micro-robot based on piezoelectric driving. *Sensors*, *18*(3), 810. https://doi.org/10.3390/s18030810

[59] International Commission on Non-Ionizing Radiation Protection. (2010). Guidelines for limiting exposure to time-varying electric and magnetic fields (1 Hz to 100 kHz). *Health Physics*, *99*(6), 818–836. https://doi.org/10.1097/HP.0b013e3181f06c86

[60] International Commission on Non-Ionizing Radiation Protection (2020). Guidelines for limiting exposure to electromagnetic fields (100 kHz to 300 GHz). *Health Physics*, *118*(5), 483–524. https://doi.org/10.1097/HP.0000000000001210

[61] Grieves, M., & Vickers, J. (2017). Digital twin: Mitigating unpredictable, undesirable emergent behavior in complex systems. In F. J. Kahlen, S. Flumerfelt, & A. Alves (Eds.), *Transdisciplinary perspectives on complex systems: New findings and approaches* (pp. 85–113). Springer. https://doi.org/10.1007/978-3-319-38756-7_4

[62] Sun, T., He, X., & Li, Z. (2023). Digital twin in healthcare: Recent updates and challenges. *Digital Health*, *9*, 20552076221149651. https://doi.org/10.1177/20552076221149651

[63] de Benedictis, A., Mazzocca, N., Somma, A., & Strigaro, C. (2023). Digital twins in healthcare: An architectural proposal and its application in a social distancing case study. *IEEE Journal of Biomedical and Health Informatics*, *27*(10), 5143–5154. https://doi.org/10.1109/JBHI.2022.3205506

[64] Haleem, A., Javaid, M., Singh, R. P., & Suman, R. (2023). Exploring the revolution in healthcare systems through the applications of digital twin technology. *Biomedical Technology*, *4*, 28–38. https://doi.org/10.1016/j.bmt.2023.02.001

[65] Mohamed, N., Al-Jaroodi, J., Jawhar, I., & Kesserwan, N. (2023). Leveraging digital twins for healthcare systems engineering. *IEEE Access*, *11*, 69841–69853. https://doi.org/10.1109/ACCESS.2023.3292119

[66] Ricci, A., Croatti, A., & Montagna, S. (2022). Pervasive and connected digital twins—A vision for digital health. *IEEE Internet Computing*, *26*(5), 26–32. https://doi.org/10.1109/MIC.2021.3052039

[67] Wickramasinghe, N., Ulapane, N., Sloane, E. B., & Gehlot, V. (2024). Digital twins for more precise and personalized treatment. In J. Bichel-Findlay, P. Otero, P. Scott, & E. Huesing (Eds.), *The future is accessible: Proceedings of the 19th world congress on medical and health informatics* (pp. 229–233). IOS Press. https://doi.org/10.3233/SHTI230961

How to Cite: Razek, A. (2025). Risk Appraisal and Protection Against the Adverse Effects of Electromagnetic Fields on Living Tissues and Near-Tissues Health Devices. *Smart Wearable Technology*, 1, A1. https://doi.org/10.47852/bonviewSWT52025846